

Precipitation from Space: Advancing Earth System Science

Paul A. Kucera¹, Elizabeth E. Ebert², F. Joseph Turk³, Vincenzo Levizzani⁴, Dalia Kirschbaum⁵, Francisco J. Tapiador⁶, Alexander Loew⁷, M. Borsche⁷

¹National Center for Atmospheric Research, Boulder, CO

²Centre for Australian Weather and Climate Research, Bureau of Meteorology, Melbourne, Victoria 3001, Australia

³Jet Propulsion Laboratory, California Institute of Technology, Pasadena, CA 91109

⁴Institute of Atmospheric Sciences and Climate, National Research Council, Bologna, Italy

⁵NASA Goddard Space Flight Center, Greenbelt, MD 20771

⁶Faculty of Environmental Sciences and Biochemistry, University of Castilla-La Mancha (UCLM), Toledo, Spain

⁷Max Planck Institute for Meteorology, 20146 Hamburg, Germany

To Be Submitted To:

Bulletin of the American Meteorological Society

19 April 2012

Revised Submission: 2 August 2012

(inset) The increasingly lengthy time span of space-based precipitation data records has enabled cross-discipline investigations and applications that would otherwise not be possible, revealing discoveries related to hydrological and land processes, climate, atmospheric composition, and ocean freshwater budget, and proving a vital element in addressing societal issues.

1. Introduction

Of the three primary sources of spatially contiguous precipitation observations (surface networks, ground-based radar, and satellite-based radar/radiometers), only the last is a viable source over ocean and much of the Earth's land. As recently as 15 years ago, users needing quantitative detail of precipitation on anything under a monthly time scale relied upon products derived from geostationary satellite thermal infrared (IR) indices (e.g., Arkin and Meisner, 1987). The Special Sensor Microwave Imager (SSM/I) passive microwave (PMW) imagers originated in 1987 and continue today with the SSM/I sounder (SSMIS) sensor. The fortunate longevity of the joint National Aeronautics and Space Administration (NASA) and Japan Aerospace Exploration Agency (JAXA) Tropical Rainfall Measuring Mission (TRMM) is providing the environmental science community a nearly unbroken data record (as of April 2012, over 14 years) of tropical and sub-tropical precipitation processes. TRMM was originally conceived in the mid-1980s (Simpson et al. 1988) as a climate mission with relatively modest goals, including monthly averaged precipitation. TRMM data were quickly exploited for model data assimilation (Hou et al. 2001) and, beginning in 1999 with the availability of near real time data, for tropical cyclone warnings (Hawkins et al. 2001).

To overcome the intermittently spaced revisit from these and other low Earth-orbiting satellites, many methods to merge PMW-based precipitation data and geostationary satellite observations have been developed, such as the TRMM Multisatellite Precipitation Product (Huffman et al., 2007) and the Climate Prediction Center (CPC) morphing method (CMORPH) (Joyce et al., 2004). The purpose of this article is not to provide a survey or assessment of these and other satellite-based precipitation datasets, which are well summarized in several recent articles (Tapiador et al., 2012; Kidd et al.,

2012; Kidd and Levizzani, 2011; Dinku et al., 2010). Rather, the intent is to demonstrate how the availability and continuity of satellite-based precipitation data records is transforming the ways that scientific and societal issues related to precipitation are addressed, in ways that would not be otherwise possible. These developments have taken place in parallel with the growth of an increasingly interconnected scientific environment. Scientists from different disciplines can easily interact with each other via information and materials they encounter online, and collaborate remotely without ever meeting each other in person. Likewise, these precipitation datasets are quickly and easily available via various data portals and are widely used. Within the framework of the NASA/JAXA Global Precipitation Measurement (GPM) (Hou et. al, 2008) mission, these applications will become increasingly interconnected.

We emphasize that precipitation observations by themselves provide an incomplete picture of the state of the atmosphere. For example, it is unlikely that a richer understanding of the global water cycle will be possible by standalone missions and algorithms, but must also involve some component of data assimilation (Michaelides et al, 2009), where model analyses of the physical state are constrained alongside multiple observations (e.g., precipitation, evaporation, radiation). The next section provides examples extracted from the many applications that use various high-resolution precipitation products. The final section summarizes the future system for global precipitation processing.

2. Applications

Precipitation products are critical for the development of applications that address a variety of scientific and societal needs. It is difficult to discuss precipitation

applications without proper consideration of the spatial and temporal scales of individual products, as well as their timeliness and veracity. The applications described below are by no means an exhaustive list, but highlight the breadth of applications that have been developed through incorporation of satellite-based precipitation datasets.

2.1 Flooding and Landslides

Floods and landslides represent some of the most devastating hydrometeorological natural disasters on Earth, resulting in extensive economic damage and fatalities that affect nearly every country in the world. Despite their broad impacts, characterizing the frequency, severity, and occurrence of such events has been primarily limited to regional or local analyses due to the dearth of rainfall gauges and the spatial scale of existing landslide and flood models. Recent research has sought to use satellite rainfall estimates from TRMM to inform the spatial and temporal distribution of flooding and landslides at the global scale (Hong et al. 2006, 2007a, 2010). These modeling efforts provide the foundation for a better understanding of the behavior, variability, and potential forecast potential of floods and rainfall-triggered landslides.

A global flood monitoring system initially developed by Hong et al. (2007b, 2010) and evaluated by Yilmaz et al. (2010) has been improved with a physically-based hydrological model (Wang et al. 2011). This Global Flood Monitoring system (GFMS) integrates TRMM Multi-Satellite Precipitation Analysis (TMPA) precipitation estimates, readily available geospatial datasets and a hydrological model running at a 1/8th degree latitude-longitude resolution. A 12-year retrospective simulation is used to develop a grid of 95th percentile routed runoff that serves as a starting point for flood detection and monitoring (Figure 1). Evaluation of this improved GFMS system against a global flood event database (Wu et al. 2012) indicates a Probability of Detection

(POD) of ~ 0.7 and a False Alarm Rate (FAR) of ~ 0.6 for floods over three days in duration. The evaluation results also suggest that basins with large dams have significantly higher FAR values, indicating the need to take into account their effects. In a similar effort, JAXA has supported the development of the Global Flood Alert System (GFAS) to support flood forecasting and warning worldwide. The system is hosted by the International Flood Network (IFNet: <http://gfas.internationalfloodnetwork.org/gfas-web/>), which provides global and regional rainfall maps of rainfall and rainfall exceedance for 5 and 10 year return periods. Other regional and global flood modeling research studies (e.g., Lettenmaier et al. 2006, Pan et al. 2010) have focused on developing hydrologic model routing schemes to improve prediction of flood onset and dissipation. These schemes have been developed and tested for several basins in the U.S. and Africa.

Rainfall-triggering landslide modeling activities have primarily utilized rainfall gauge information and can generally be divided into three categories: static approaches to characterize the spatial distribution of potentially susceptible areas; regional empirical approaches that evaluate the intensity and duration of rainfall in potentially triggering a landslide event; and site-specific deterministic approaches where a slope-stability model is applied to characterize the specific nature of landslide processes at the hillslope scale. A prototype landslide algorithm developed by Hong et al. (2006, 2007a) couples a static landslide susceptibility map with TMPA rainfall information to indicate areas that may be prone to landslides at the global scale. The algorithm is updated every three hours and provides landslide nowcasts from 50°N to 50°S at a 0.25° x 0.25° pixel resolution. Evaluation of this prototype system suggests that the current susceptibility map and rainfall thresholds employed show some skill (POD ranged from a maximum 22% for

1-day temporal window and minimum of 6% for 7-day temporal window for the two years evaluated) in identifying landslide-prone regions, but also serve to over or under estimate landslide nowcasting in several regions (Kirschbaum et al. 2009). Results also indicate that this system would be enhanced if precipitation characteristics of landslide-triggering events are considered within different climatologic zones to better account for the variability of rainfall intensity and duration (Kirschbaum et al. 2011). The higher resolution precipitation observations and corresponding surface conditions would better resolve localized landslide hazards (e.g., topography, soil conditions) that are not observed in the coarse scale global landslide algorithm.

In the abovementioned flood and landslide modeling approaches, the near real-time accessibility and global availability of the TRMM and future GPM products enables rapid hazard assessment and potential flood and landslide forecasting. Real-time products can be accessed at

http://trmm.gsfc.nasa.gov/publications_dir/potential_flood_hydro.html. While the current spatial resolution of the TRMM products generally restricts their application to the scale of the TRMM products (0.25° x 0.25°, 3-h), results indicate that using satellite-based precipitation products enables the characterization of flood and landslide hazards at the global scale, filling much needed gap in the hazard assessment community. As the resolution of the precipitation products improve, the model resolution should also improve, providing better information of flood and landslide hazards at finer scales.

2.2 Ensemble Tropical Rainfall Potential

Heavy rains associated with landfalling tropical cyclones frequently trigger floods that cause millions of dollars of damage and lost lives. To provide observations-based

forecast guidance for tropical cyclone (TC) heavy rain, Kidder et al. (2005) developed the Tropical Rainfall Potential (TRaP), an extrapolation forecast generated by accumulating rainfall estimates from microwave sensors over a 24-hour period as the storm is translated along the forecast track. TRaP aims to predict the maximum rainfall at landfall, as well as the spatial pattern of precipitation, and has been shown to have similar or better skill than short-range numerical weather prediction models (Ferraro et al. 2005, Ebert et al. 2005).

One key aspect where satellite-based precipitation products excel is their relative skill in the location and timing of precipitation. The issue of assimilating precipitation observations (or precipitation-affected satellite radiances) into weather prediction models is yet an open topic of investigation (Bauer et al., 2011). A recent innovation has been to combine the TRaP forecasts from multiple sensors and various start times into an ensemble TRaP product known as eTRaP (Ebert et al. 2011). The ensemble approach provides not only more accurate quantitative precipitation forecasts, including more skilful maximum rainfall amount and location, it also produces probabilistic forecasts of rainfall exceeding various thresholds that decision makers can use to make critical risk assessments. Ebert et al. (2011) showed that eTRaP probabilistic forecasts have useful skill, but the grid-scale probabilities are biased high when compared to observations and should be interpreted in a broader spatial context. Efforts to calibrate the probabilistic forecasts from eTRaP are underway. Figure 2 shows an example of an eTRaP forecast for Typhoon Muifa as it passed south of Okinawa on 4 August 2011. It predicted 50% probability of exceeding 100 mm over northern Okinawa, with a maximum 24 h rainfall of about 300 mm. The measured 24 h rainfall at 12 UTC on 5 August was 147.5 mm at Oku on the northern tip of Okinawa, and 313.5 mm at Nago in

the center of the island. While the location of the maximum rain in the eTRaP forecasts was spatially displaced by about 50 km, it would have provided useful guidance for forecasters and emergency managers.

ETRaPs are computed four times daily for all named tropical cyclones and storms, and can be viewed at <http://www.ssd.noaa.gov/PS/TROP/etrap.html>.

2.3 Global high resolution terrestrial surface heat and moisture flux estimates

Evapotranspiration is one of the major fluxes in the hydrological cycle. The latent heat flux (LE) amounts to about 80 W m^{-2} (Trenberth et al. 2009) on global scale (ocean and land) and is therefore the largest single heat source for the atmosphere with high relevance in weather and global water cycle dynamics (Dirmeyer 2006). However, existing data sets of surface heat fluxes are still highly uncertain. The GEWEX LandFluxEval project focused on the comparison of a variety of different existing LE products over land. A spread of 20 W m^{-2} ($\sigma=5 \text{ W m}^{-2}$) was identified between different existing datasets, with an all-product global mean value of 45 W m^{-2} for the land surface latent heat flux (Jimenez et al. 2011; Mueller et al. 2011). These uncertainties are comparably large when compared to global scale heat fluxes and correspond to roughly one-third of the annual global sensible heat flux of 17 W m^{-2} (Trenberth et al., 2009).

The availability of accurate global precipitation data is one major driver for an accurate determination of surface heat fluxes as it is major input for land surface models used to estimate surface heat fluxes. Currently, only satellite data can provide precipitation

estimates at the global scale with sufficient temporal resolution. Miralles et al. (2011) used CMORPH (Joyce et al. 2004) and the Global Precipitation Climatology Program (GPCP) (Huffman et al. 2009) daily precipitation for the generation of a global dataset of evapotranspiration with a spatial resolution of 0.25 degrees.

Borsche and Loew (2012) have analyzed the impact of using satellite based precipitation estimates for the estimation of surface latent heat fluxes using spatially and temporally high resolution geostationary satellite data for surface radiation fluxes and TMPA for precipitation estimates (Knapp et al. 2011). They analyzed the impact of replacing rain gauge based precipitation data by TMPA 3-hourly rainfall intensities (Huffman et al. 2007) for the estimation of surface latent heat fluxes through a series of experiments and validating the estimated surface heat fluxes by in situ measurements from FluxNet (Aubinet et al. 1999; Baldocchi 2008). Figure 3 shows the seasonal mean latent heat flux as estimated from geostationary observations using TMPA precipitation as forcing. Figure 4 shows the correlation and root-mean squared error (RMSE) of estimated and observed latent heat fluxes for 19 different FluxNet stations from different biomes using either only station data as a forcing or satellite based forcing. The RMSE is 56.8 and 63.6 W m^{-2} at hourly timescales for station and satellite based forcing respectively. At daily timescales the RMSE is 39.0 (43.1) W m^{-2} for station (satellite) forcing. While the errors for the satellite based LE estimates are slightly higher than for the station forcing, Borsche and Loew (2012) show that this increase in uncertainty is mainly due to uncertainties in the radiation forcing and less due to uncertainties in the available TMPA precipitation data.

A related application involves the close correspondence between soil moisture and precipitation. Soil moisture controls the partitioning of precipitation into infiltration, surface runoff, and evaporation/ transpiration from land surfaces. The precipitation time history also modulates the microwave surface emissivity, an important consideration for over-land precipitation estimation (Li et. al., 2010). Comparisons of surface emissivity retrievals together with the previous-time precipitation totals are an indirect yet qualitative way to validate emissivity retrievals over rain-affected surfaces, and to devise improved over-land precipitation retrievals (Ferraro et al. 2012). Another application that uses satellite precipitation products to compute representative land surface conditions (e.g., soil moisture) is the Modern-Era Retrospective Analysis for Research (MERRA) project (Reichle et. al, 2011), which is generated by the NASA Global Modeling and Assimilation Office (GMAO: <http://gmao.gsfc.nasa.gov/>). MERRA focuses on the assimilation of in situ and remote sensing data into numerical models to provide a representative global atmospheric (e.g., precipitation, temperature, humidity) and land surface dataset (e.g., soil moisture, snow, runoff). The MERRA products are then used for a variety of applications such as the study of land surface water budgets including floods, droughts, soil moisture processes. Having accurate satellite precipitation data increases the usefulness of datasets such as MERRA by reducing the uncertainty of the generated fields.

2.4 Atmospheric Aerosols

Aerosol particles introduce one of the largest uncertainties in model-based estimates of direct and indirect forcing on climate. Aerosol processes in models such as transport, source, and sinks typically rely on model-derived meteorology and are assimilated into operational aerosol prediction models (Zhang et al., 2008). However, the processes are sensitive to errors in the underlying simulation that propagate through the system.

Precipitation, as one of the basic meteorological elements in an aerosol model, has a large effect on aerosol load since it is the primary sink. It is expected that precipitation area coverage is more important than precipitation intensity in affecting model aerosol optical thickness (AOT), but a potential implication is that excessive light precipitation in models (Sun et al. 2006) may over-scavenge aerosol particles.

Xian et al. (2009) found that light rain over large areas using the Navy Operational Global Atmospheric Prediction System (NOGAPS) forecast model removed significantly more aerosol particles than the more realistic heavy rain in small areas found in the NRL-Blend satellite precipitation product (Turk and Miller, 2005), even though the total precipitation was nearly the same in the two schemes. Figure 5 shows the smoke AOT resulting from the use of the NRL-Blend precipitation in the tropics on the left, and the ratio of smoke AOT NRL-Blend run over NOGAPS run on the right for four burning seasons. When NRL-Blend precipitation is used instead of NOGAPS, smoke AOT in general increases in the tropics for all seasons including the least active burning period, November through January. During February through April, which is the major burning period for peninsular Southeast Asia, the increase in AOT with the NRL-Blend run is about a factor of two on average, and up to 2.8 over Malaysia Peninsula. Thus while on seasonal time scales current numerical models could approximately capture the real world precipitation pattern, there might exist differences in regional AOT due to differences in short time scale precipitation. This could significantly affect wet deposition of aerosols, and thus modeled AOT in regions of convection. Other short time scale problems, such as trying to infer aerosol concentrations in the vicinity of convective cells observed by satellite, may also be challenged by the model's precipitation scheme. Aerosol particles may be overly

scavenged out in the model by the time the air mass reaches the observed cell (Turk and Xian 2012).

2.5 Model assessment and validation

Unlike prognostic variables such as temperature and moisture, precipitation is a diagnosed quantity in most weather and climate models. Owing to the methods whereby precipitation is triggered, it is not only important to verify model-derived precipitation quantitatively (Ebert et al., 2005), but also the capability of the model to place precipitation in the right place at the right time. In this regard, satellite precipitation datasets are the pillars for validating the performance of numerical models such as Regional Climate Models (RCMs), which are dynamically downscaling tools used to improve the spatial resolution of outputs from reanalyses and Global Climate Models (GCM). Over land, several studies have shown that RCMs provide consistent estimates of precipitation after accounting for known uncertainties in the reference data (Tapiador, 2010). Gauge data, such as the Climate Research Unit (CRU), GPCP, the Climate Prediction Center (CPC) Merged Analysis of Precipitation (CMAP), and the Global Precipitation Climatology Center (GPCC) databases have been compared with RCM simulations over Europe both in terms spatially reproducing the climatology and the probability distributions of precipitation (Tapiador et al., 2009), and in terms of capturing the phase and power of precipitation cycles (Tapiador and Sánchez, 2008), obtaining consistent results. Such intercomparison / validation of RCMS is directly relevant for applications such as hydropower since RCMs outputs are used to gauge the future availability of water for this renewable energy (Tapiador 2009, Tapiador et al. 2012).

Over the oceans, however, there are no or few rain gauges available, so satellite observations are needed to validate models. Measuring and modeling oceanic precipitation is important since this geophysical parameter is required for a full understanding of the Earth System, including the closure of the hydrological cycle. Comparisons of RCMs outputs with satellite-based databases (Figure 6) such as the GPCP (Adler et al., 2003) are instrumental to evaluate the performances of the RCMs over the oceans, and thus to improve the models.

2.6 Societal Impact Monitoring

Soil moisture controls the partitioning of precipitation into infiltration and surface runoff, and satellite precipitation records provide observations to better understand the spatiotemporal link between precipitation and soil moisture. Many of the same PMW sensors used for precipitation estimation can be adapted for use in estimating soil moisture and vegetation water content (Li et. al, 2010). Soil moisture products are used to augment gauge sparse areas to improve short-term precipitation estimates (Crow et. al., 2009). Satellite precipitation estimates have been critical for monitoring of drought in Africa where surface observations are sparse. For example, Fig. 7 shows the 2011 precipitation anomaly for March-April-May for the southern two-thirds of Africa compared to the 2000-2009 climatology. The map shows areas that were prone to drought (e.g., East Africa) and or flooding (e.g., South Africa) during this period. In a changing climate scenario, droughts are perhaps the less known part of the water cycle especially in those areas that are more exposed than others to the drought risk, such as the Horn of Africa (Lyon and De Witt, 2012).

To address the issues of water availability (or lack of) and predictions of future water scarcity in the context of global climate change, the project Global Water Monitoring Information Service (GLOWASIS) of the 7th Framework Programme of the European Commission uses satellite rainfall estimations for the hydrological monitoring and forecasting in the context of the Global Monitoring for Environment and Security (GMES) initiative (<http://glowasis.eu/>). Because accurate estimates of water availability in remote areas such as Africa are difficult to obtain, but are critical for monitoring crop production and associated issues with food security, GLOWASIS has focused on improving the quantification of errors in water budget components, global models and space-based global precipitation measurements. This effort is in attempt to increase the accuracy of monthly forecasts of water availability. The GLOWASIS project is attempting to meet the challenges of addressing the monitoring water availability by combining models with observations (e.g., satellite precipitation products) through improved algorithms. These resources are available to regional decision makers through open access to the products. The GLOWASIS project is one example of an application the requires satellite precipitation products to improve the monitoring to help improve in the preparation of regional to global impacts on society such as droughts and floods.

3. Conclusions

This article has highlighted several cross-disciplinary Earth system science investigations that have been advanced through the availability of consistent global precipitation records. An increasing number of applications are dependent upon the availability of near real-time information that may not be science-quality data; others require science-quality data records that are hosted by distributed data archive centers. The planned and future satellite missions are critical for the continued advancement of

precipitation products and subsequently, applications that utilize the precipitation products. These new satellite missions will overlap with existing satellite missions to provide consistent, long-term data records.

The global constellation of Earth observing systems for precipitation is constructed with a variety of instruments, low Earth orbiting microwave imagers and sounders, radar, and geostationary Earth orbiting imagers. Community efforts such as the Global Satellite Intercomparison (GSICS; Goldberg et al. 2011) are imperative to establish self-consistent data records across satellite lifetimes, sensor revisions, etc. The space-based precipitation observing system was recently enhanced by the deployment of the joint French National Space Study Center (CNES) and Indian Space Research Organization (ISRO) Megha-Tropiques satellite (orbiting asynchronously in a 20-degree inclination), the first of an advanced microwave sounder (ATMS) onboard the Suomi National Polar Orbiting Partnership (NPP) spacecraft, JAXA's Global Change Observing Mission (GCOM-W), and the Chinese Meteorological Agency (CMA) FY-3 series. Currently, TRMM is well beyond its expected life but will continue to collect observations until it exhausts its station-keeping fuel supply (largely determined by the solar cycle), after which it will begin its gradual deorbit. However, there is a possibility that TRMM will overlap with the upcoming (2014) GPM mission, providing an opportunity for a seamless, longterm data record. The core GPM spacecraft will deploy an advanced dual-frequency (Ku/Ka-band) precipitation radar (DPR) orbiting at a 65-degree orbit inclination, providing coverage at high latitudes not overflowed by by TRMM for estimation of snowfall and light precipitation. The GPM core satellite will be joined by NASA's Soil Moisture Active Passive (SMAP) satellite in 2015, enabling

complementary measurements and synergistic analyses between surface soil moisture state and precipitation (Entekhabi et al., 2010).

A future global precipitation processing system will likely encompass multiple satellite sensors (active and passive), ground observations and radar networks to obtain improved spatial and temporal resolution with reduced uncertainties. For example, flash flood guidance systems need short time scale, high resolution precipitation fields, especially in remote regions, to improve flash flood forecasting on a basin scale. Societal applications such as drought monitoring, soil moisture/crop monitoring, and health monitoring (e.g., meningitis outbreaks in Africa) can benefit from satellite precipitation datasets. Large-scale applications such as regional climate modeling will benefit from the higher resolution precipitation data when evaluating potential climate impacts at a regional scale.

4. Acknowledgements

This paper was facilitated through numerous discussions with International Precipitation Working Group (IPWG: <http://www.isac.cnr.it/~ipwg/IPWG.html>) members (Kidd et al, 2010). We acknowledge Dr. Peng Xian from the Naval Research Laboratory, Monterey for her assistance with the atmospheric composition section. This paper is dedicated to David I.F. Grimes (1951-2011), who was an advocate for development and outreach of precipitation products to meet societal needs in Africa.

5. References

- Adler, Robert F., et al., 2003. The version-2 Global Precipitation Climatology Project (GPCP) monthly precipitation analysis (1979–present). *Journal of Hydrometeorology*, **4**, 1147–1167.
- Arkin, P. A., and B. N. Meisner, 1987: The relationship between large-scale convective rainfall and cold cloud over the western hemisphere during 1982-84, *Mon. Wea. Rev.*, **115**, 51-74.
- Aubinet, M., A. Grelle, A. Ibrom, A. Rannik, J. Moncrieff, T. Foken, A. Kowalski, P. Martin, P. Berbigier, C. Bernhofer, R. Clement, J. Elbers, A. Granier, T. Grünwald, K. Morgenstern, K. Pilegaard, C. Rebmann, W. Snijders, R. Valentini, and T. Vesala, 1999: Estimates of the annual net carbon and water exchange of forests: The Euroflux methodology. *Advances in Ecological Research*, **30**, 113 – 175.
- Baldocchi, D., 2008: Breathing of the terrestrial biosphere: Lessons learned from a global net-work of carbon dioxide flux measurement systems. *Australian Journal of Botany*, **56**, 1 – 26.
- Bauer, P., G. Ohring, C. Kummerow, and T. Auligne, 2011: Assimilating satellite observations of clouds and precipitation into NWP models. *Bull. Amer. Meteor. Soc.*, **92**, ES25–ES28. doi: <http://dx.doi.org/10.1175/2011BAMS3182.1>
- Borsche, M. and A. Loew, 2012: Estimating land surface heat fluxes from satellite data – an uncertainty assessment. In review.
- Crow, W.T., G.J. Huffman, R. Bindlish, and T.J. Jackson, 2009: Improving Satellite-Based Rainfall Accumulation Estimates Using Spaceborne Surface Soil Moisture Retrievals. *J. Hydrometeor.*, **10**, 199–212.
- Dinku, T., F. Ruiz, S.J. Connor, P. Ceccato, 2010: Validation and intercomparison of satellite rainfall estimates over Colombia. *J. Appl. Meteor. Climatol.*, **49**, 1004–1014.
- Dirmeyer, P., 2006: The Hydrologic Feedback Pathway for Land–Climate Coupling. *J. Hydro.*, **7**, 857–867.
- Ebert, E.E., J.E. Janowiak, and C. Kidd, 2007: Comparison of near real time precipitation estimates from satellite observations and numerical models. *Bull. Amer. Met. Soc.*, **88**, 47-64.
- Ebert, E., S. Kusselson and M. Turk, 2005: Validation of NESDIS operational tropical rainfall potential (TRaP) forecasts for Australian tropical cyclones. *Aust. Meteorol. Mag.*, **54**, 121-135.
- Ebert, E.E., M. Turk, S.J. Kusselson, J. Yang, M. Seybold, P.R. Keehn, R.J. Kuligowski, 2011: Ensemble tropical rainfall potential (eTRaP) forecasts. *Wea. Forecasting*, **26**, 213-224.
- Entekhabi, D., E. Njoku, P. O'Neill, K. Kellogg, W. Crow, W. Edelstein, J. Entin, S. Goodman, T. Jackson, J. Johnson, J. Kimball, J. Piepmeier, R. Koster, K. McDonald, M. Moghaddam, S. Moran, R. Reichle, J. C. Shi, M. Spencer, S. Thurman, L. Tsang, and J. Van Zyl, 2010: The Soil Moisture Active and Passive (SMAP) Mission. *Proceedings of the IEEE*, **98(5)**, 704-716, 10.1109/JPROC.2010.2043918, 2010.

- Ferraro, R.R., C. Peters-Lidard, C. Hernandez, Turk, F.J., Aires, F., Prigent, C., Xin, L., Boukabara, S-A., Furuzawa, F., Gopalan, K., Harrison, K., Karbou, F., Li, L., Liu, C., Masunaga, H., Moy, L., Ringerud, S., Skofronick-Jackson, G., Tian, Y., Wang, N-Y., 2012: An evaluation of microwave land surface emissivities over the continental United States to benefit GPM-era precipitation algorithms. *IEEE Trans. Geosci. Rem. Sens*, accepted.
- Ferraro, R., P. Pellegrino, M. Turk, W. Chen, S. Qiu, R. Kuligowski, S. Kusselson, A. Irving, S. Kidder and J. Knaff, 2005: The Tropical Rainfall Potential (TRaP) technique. Part 2: Validation. *Wea. Forecasting*, **20**, 465-475.
- Goldberg, M., G. Ohring, J. Butler, C. Cao, R. Datla, D. Doelling, V. Gartner, T. Hewison, B. Iacovazzi, D. Kim, T. Kurino, J. Lafeuille, P. Minnis, D. Renaut, J. Schmetz, D. Tobin, L. Wang, F. Weng, X. Wu, F. Yu, P. Zhang, and T. Zhu, 2011: The global space-based inter-calibration system. *Bull. Amer. Meteor. Soc.*, **92**, 467-475.
- Hawkins, J D, T F Lee, J Turk, C Sampson, J Kent, and K Richardson, 2001: Real-time internet distribution of satellite products for tropical cyclone reconnaissance. *Bull. Amer. Meteor. Soc.*, **82**, 567-578.
- Hong, Y., R. Adler, and G. Huffman, 2006: Evaluation of the potential of NASA multi-satellite precipitation analysis in global landslide hazard assessment. *Geophysical Research Letters*, **33**(L22402), 1-5. doi:10.1029/2006GL028010.
- Hong, Y., R. Adler, and G. Huffman, 2007a: Use of satellite remote sensing data in the mapping of global landslide susceptibility. *Natural Hazards*, **43**(2), 245-256. doi:10.1007/s11069-006-9104-z.
- Hong, Y., R. F. Adler, F. Hossain, S. Curtis, and G. J. Huffman, 2007b: A first approach to global runoff simulation using satellite rainfall estimation. *Water Resources Research*, **43**(W08502). doi:10.1029/2006WR005739.
- Hong, Y., R. Adler, and G. Huffman, 2010: Applications of TRMM-based Multi-satellite Precipitation Estimation for Global Runoff Simulation: Prototyping a Global Flood Monitoring System. In F. Hossain & M. Gebremichael (Eds.), *Satellite Applications for Surface Hydrology* (p. 327). Springer Verlag.
- Hou, A. Y., S. Q. Zhang, A. M. da Silva, W. S. Olson, C. D. Kummerow, and J. Simpson, 2001: Improving global analysis and short-range forecast using rainfall and moisture observations derived from TRMM and SSM/I passive microwave sensors. *Bull. Amer. Meteor. Soc.*, **82**, 659-680.
- Hou, A., G. S. Jackson, C. Kummerow, C. M. Shepherd, 2008. Chapter 6 in Global precipitation measurement. In: Silas, Michaelides (Ed.), *Precipitation: Advances in Measurement, Estimation, and Prediction*. Springer Publishers, pp. 131–164.
- Huffman, G. J., R. F. Adler, D. T. Bolvin, G. Gu, 2009: Improving the Global Precipitation Record: GPCP Version 2.1. *Geophys. Res. Lett.*, **36**, L17808, doi:10.1029/2009GL040000.
- Huffman, G. J., R. F. Adler, D. T. Bolvin, G. Gu, E. J. Nelkin, K. P. Bowman, E. F. Stocker, and D. B. Wolff, 2007: The TRMM Multi-satellite Precipitation Analysis: Quasi-Global Multi-Year Combined-Sensor Precipitation Estimates at Fine Scale. *J. Hydrometeor.*, **8**, 38-55.

- Jimenez, C., C. Prigent, B. Mueller, S. I. Seneviratne, M. F. McCabe, E. F. Wood, W. B. Rossow, G. Balsamo, A. K. Betts, P. A. Dirmeyer, J. B. Fisher, M. Jung, M. Kanamitsu, R. H. Reichle, M. Reichstein, M. Rodell, J. Sheffield, K. Tu, and K. Wang, 2011: Global intercomparison of 12 land surface heat flux estimates. *J. Geophys. Res.*, **116**, D02102, doi:10.1029/2010JD014545.
- Joyce, R. J., J. E. Janowiak, P. A. Arkin, and P. Xie, 2004: CMORPH: A method that produces global precipitation estimates from passive microwave and infrared data at high spatial and temporal resolution, *J. Hydrometeor.*, **5**, 487–503.
- Kidd, C., P. Bauer, J. Turk, G. J. Huffman, R. Joyce, K.-L. Hsu, and D. Braithwaite, 2012: Intercomparison of high-resolution precipitation products over northwest Europe. *J. Hydrometeorology*, **13**, 67-82.
- Kidd, C., and V. Levizzani, 2011: Status of satellite precipitation retrievals. *Hydrol. Earth Syst. Sci.*, **15**, 1109-1116.
- Kidd, C., R. R. Ferraro, and V. Levizzani, 2010: The Fourth International Precipitation Working Group Workshop. *Bull. Amer. Meteor. Soc.*, **91**, 1095-1099.
- Kidder, S.Q., S.J. Kusselson, J.A. Knaff, R.R. Ferraro, R.J. Kuligowski, and M. Turk, 2005: The Tropical Rainfall Potential (TRaP) technique. Part 1: Description and examples. *Wea. Forecasting*, **20**, 456-464.
- Kirschbaum, D. B., R. Adler, Y. Hong, and A. Lerner-Lam, 2009: Evaluation of a preliminary satellite-based landslide hazard algorithm using global landslide inventories. *Natural Hazards and Earth System Sciences*, **9**, 673-686.
- Kirschbaum, D. B., R. Adler, Y. Hong, S. Kumar, C. Peters-Lidard, and A. Lerner-Lam, 2011: Advances in landslide nowcasting: evaluation of a global and regional modeling approach. *Environmental Earth Sciences*. doi:10.1007/s12665-011-0990-3.
- Knapp, K. R., S. Ansari, C. L. Bain, M. A. Bourassa, J. Michael; C. Funk, C. N. Helms, C. C. Hennon, C. D. Holmes, G. J. Huffman, J. P. Kossin, H.-T. Lee, A. Loew, and G. Magnusdottir, 2011: Globally gridded satellite (GridSat) observations for climate studies. *Bull. Amer. Meteor. Soc.*, **92**, 893-907.
- Lettenmaier, D.P, A. de Roo, and R. Lawford, 2006: Towards a capability for global flood forecasting. *Bulletin: The Journal of the World Meteorological Organization*, **55**(3), 185-190.
- Li, L., P.W. Gaiser, B.C. Gao, R.M. Bevilacqua, T.J. Jackson, E.G. Njoku, C. Rudiger, J.C. Calvet, and R. Bindlish, 2010: WindSat global soil moisture retrieval and validation. *IEEE Trans. Geosci. Rem. Sens.*, **48**, no. 5, 2224-2241.
- Lyon, B., and D. G. DeWitt, 2012: A recent and abrupt decline in the East African long rains. *Geophys. Res. Lett.*, **39**, L02702, doi:02710.01029/02011GL050337.
- Michaelides, S., V. Levizzani, E. N. Anagnostou, P. Bauer, T. Kasparis, and J. E. Lane, 2009: Precipitation: Measurement, remote sensing, climatology and modeling. *Atmos. Res.*, **94**, 512-533.
- Miralles, D. G., T. R. H. Holmes, R. A. M. De Jeu, J. H. Gash, A. G. C. A. Meesters, A. J. Dolman, 2011: Global land-surface evaporation estimated from satellite-based observations *Hydrology and Earth System Sciences, Copernicus Publications*, **15**, 453-469.

- Mueller, B., S.I. Seneviratne, C. Jimenez, T. Corti, M. Hirschi, G. Balsamo, P. Ciais, P. Dirmeyer, J.B. Fisher, Z. Guo, M. Jung, F. Maignan, M.F. McCabe, R. Reichle, M. Reichstein, M. Rodell, J. Sheffield, A. J. Teuling, K. Wang, E.F. Wood, and Y. Zhang, 2011: Evaluation of global observations-based evapotranspiration datasets and IPCC AR4 simulations. *Geophysical Research Letters*, **38**, L06402, doi:10.1029/2010GL046230.
- Pan, M., H. Li, and E. F. Wood, 2010: Assessing the Skill of Satellite-based Precipitation Estimates in Hydrologic Applications, *Water Resources Research*, **46**, W09535, doi:10.1029/2009WR008290.
- Reichle, Rolf. H., R. D. Koster, G. J. M. DeLannoy, B. A. Forman, Q. Liu, P. P. Mahanama, and A. Toure, 2011: Assessment and Enhancement of MERRA Land Surface Hydrology Estimates. *J. Climate*, **24**, 6322-6338, DOI: 10.1175/JCLI-D-10-05033.1.
- Simpson, J., R.F. Adler, and G. North, 1988: A proposed Tropical Rainfall Measuring Mission (TRMM) satellite. *Bull. Amer. Meteor. Soc.*, **69**, 278-295.
- Solomon, S. et al. (2007), *Climate Change 2007: The Scientific Basis, An Evaluation of the IPCC (International Panel on Climate Change)*, Cambridge Univ. Press, New York.
- Sun, Y., S. Solomon, A. Dai and R. W. Portmann, 2006: How often does it rain? *J. of Climate*, **19**, 916-934.
- Tapiador, F. J., and Coauthors, 2012: Global precipitation measurement: Methods, datasets and applications. *Atmos. Res.*, **104-105**, 70-97.
- Tapiador, F.J., 2010: A joint estimate of the precipitation climate signal in Europe using eight regional models and five observational datasets. *J. of Climate*, **23**, 1719-1738.
- Tapiador, F.J., E. Sánchez and R. Romera, 2009: Exploiting an ensemble of regional climate models to provide robust estimates of projected changes in monthly temperature and precipitation probabilistic distribution functions. *Tellus-A*, **61**, 57-71 DOI: 10.1111/j.1600-0870.2008.00374.x.
- Tapiador, F.J. and E. Sánchez, 2008: Changes in the European precipitation climatologies (2070-2100) as derived by eight regional climate models. *J. of Climate*, **21**, 2540-2557.
- Trenberth, K. E., J. T. Fasullo, J. Kiehl, 2009: Earth's Global Energy Budget. *Bull. Amer. Meteor. Soc.*, **90**, 311-323.
- Turk, F.J., and P. Xian, 2012: An assessment of satellite-based, high-resolution precipitation datasets for atmospheric composition studies in the Maritime Continent. *Atmos. Research*, accepted.
- Turk, F.J., and S.D. Miller, 2005: Toward Improving Estimates of Remotely-Sensed Precipitation with MODIS/AMSR-E Blended Data Techniques. *IEEE Trans. Geosci. Rem. Sens.*, **43**, 1059-1069.
- Wang, J., H. Yang, L. Li, J. J. Gourley, I. K. Sadiq, K. K. Yilmaz, R. F. Adler, F. S. Policelli, S. Habib, D. Irwin, A. S. Limaye, T. Korme, and L. Okello, 2011: The coupled routing and excess storage (CREST) distributed hydrological model. *J. Hydrol. Sci.*, **56**(1), 84-98.

- Wu, H., R. Adler, Y. Tian, Y. Hong, F. Policelli, 2012: Evaluation of Global Flood Detection Using Satellite-based Rainfall and a Hydrological Model. *J. Hydromet.* doi:10.1175/JHM-D-11-087.1.
- Yilmaz, K. K., R. F. Adler, Y. Tian, Y. Hong, and H. F. Pierce, 2010: Evaluation of a satellite-based global flood monitoring system. *International Journal of Remote Sensing*, **31**(14), 3763-3782. doi:10.1080/01431161.2010.483489.
- Xian, P., J. S. Reid, F.J. Turk, D.L. Westphal, E.J. Hyer, T.F. Hogan, 2009: Impact of modeled versus satellite measured tropical precipitation on wet removal in an aerosol transport model. *Geophys. Res. Letters*, **36**, doi:10.1029/2009GL038823.
- Zhang, J., J. S. Reid, D. L. Westphal, N. L. Baker, and E. J. Hyer, 2008: A system for operational aerosol optical depth data assimilation over global oceans. *J. Geophys. Res.*, **113**, D10208, doi:10.1029/2007JD009065.

List of Figures

Figure 1: Water depth over 95th percentile of 12-year simulation of routed runoff as initial indicator of flooding in Global Flood Monitoring System. Example of real-time results for Australian floods in January 2011.

Figure 2: ETRaP forecast of (a) probability of 24 h precipitation exceeding 100 mm, and (b) 24 h rain accumulation in Typhoon Muifa, valid at 12 UTC on 5 August 2011.

Figure 3: Seasonal (JJA) high resolution (5 km) mean latent heat derived from geostationary satellite data using TMPA precipitation data (Borsche and Loew, 2011).

Figure 4: Multiannual RMSE difference and correlation of latent heat flux obtained from station forcing (left) and satellite forcing (right) using different FluxNet stations as a reference. Different colors correspond to different temporal aggregation (Borsche and Loew, 2012).

Figure 5: Left: Smoke AOT resulted from NRL-blend precipitation for four biomass burning periods in 2007. Right: Ratio of smoke AOT resulted from NRL-blend precipitation over smoke AOT resulted from NOGAPS precipitation for four biomass burning periods in 2007 (colored for regions with AOT > 0.05 in NRL-blend run) (Xian et al. 2009).

Figure 6: Comparison of the ensemble average of eight Regional Climate Models (RCMs, 0.5° resolution) with a satellite-based observational database (GPCP, 2.5° resolution) over Europe, for present-day climatologies. The difference plots (third column) illustrate the contrasting performances of the RCMs depending on season and on location. Note the different spatial resolution of the data, which affects maxima and minima.

Figure 7: African 2011 March-April-May (MAM) rainfall anomaly relative to 2000-2009 climatology.

Australian Floods January 2011

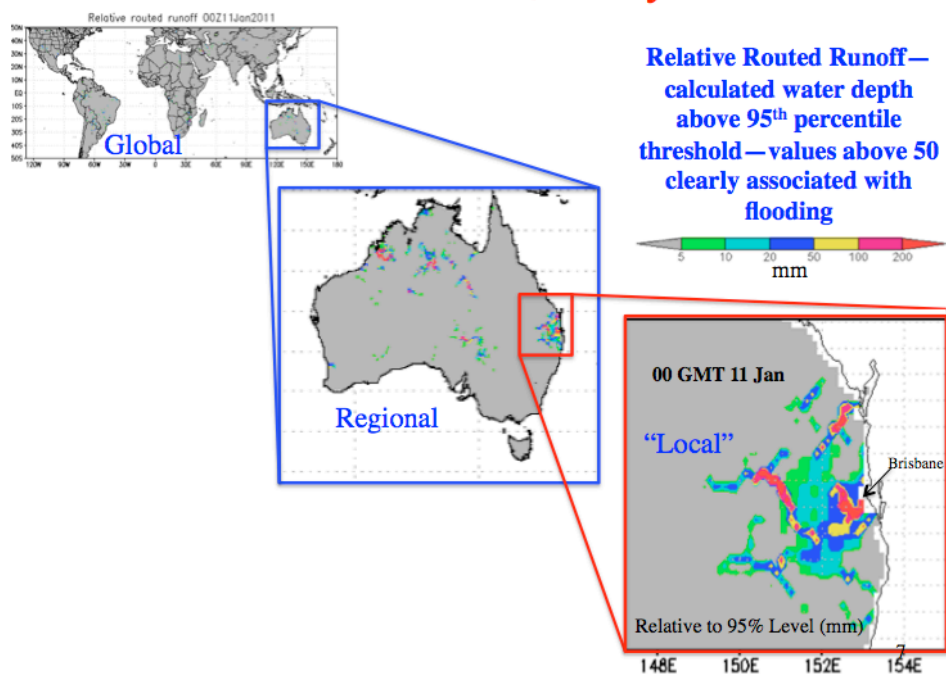


Figure 1: Water depth over 95th percentile of 12-year simulation of routed runoff as initial indicator of flooding in Global Flood Monitoring System. Example of real-time results for Australian floods in January 2011.

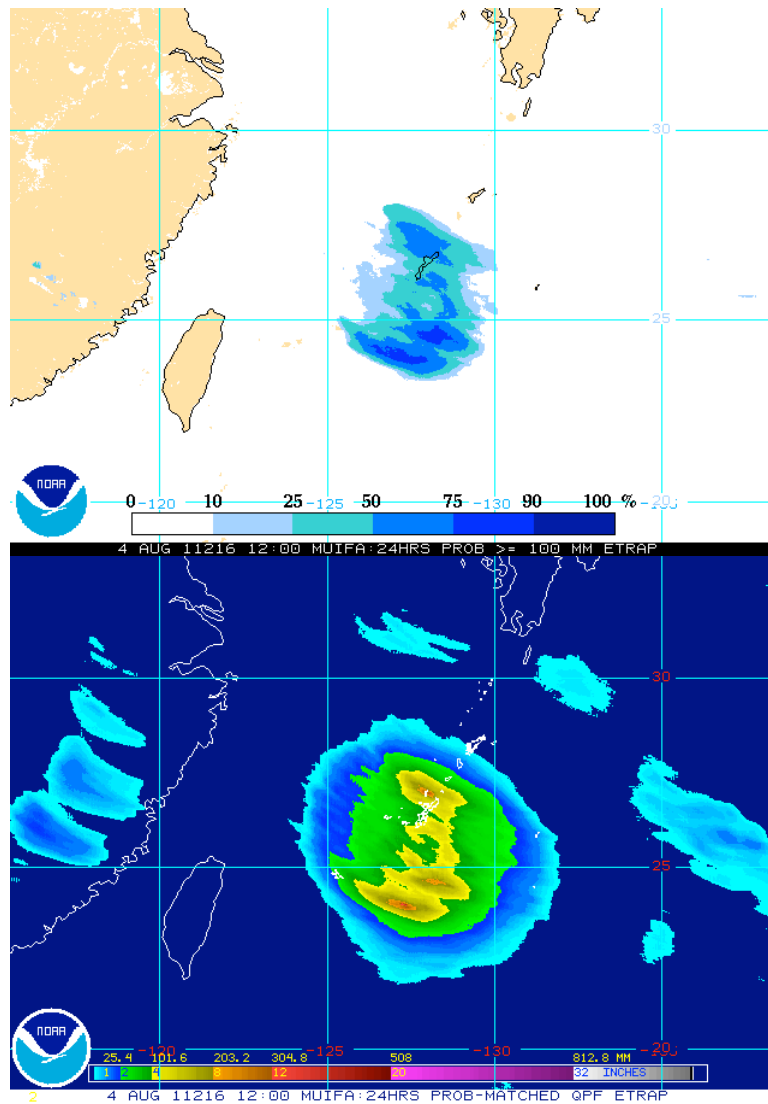


Figure 2: ETRaP forecast of (a) probability of 24 h precipitation exceeding 100 mm, and (b) 24 h rain accumulation in Typhoon Muifa, valid at 12 UTC on 5 August 2011. ETRaPs are computed four times daily for all named tropical cyclones and storms, and can be viewed at <http://www.ssd.noaa.gov/PS/TROP/etrap.html>.

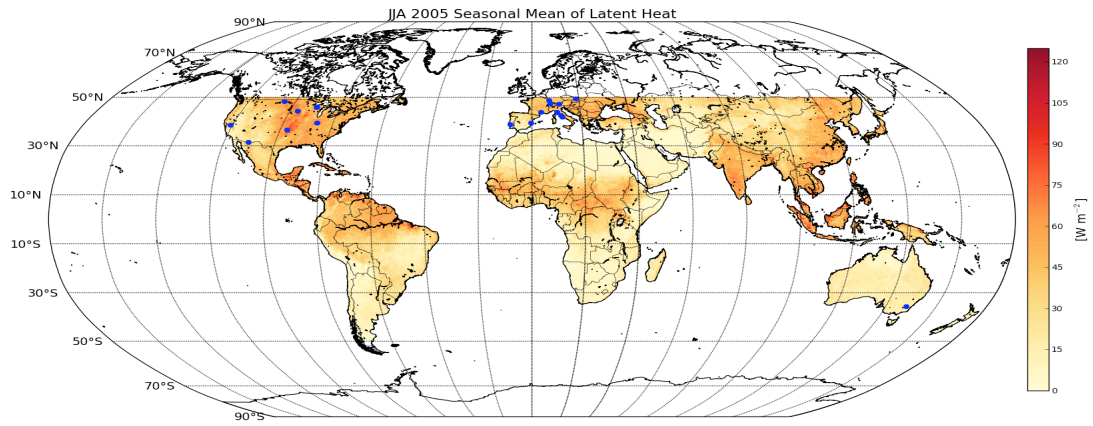


Figure 3: Seasonal (JJA) high resolution (5 km) mean latent heat derived from geostationary satellite data using TMPA precipitation data. Blue circles correspond to FluxNet stations shown in Figure 4 (Borsche and Loew 2011).

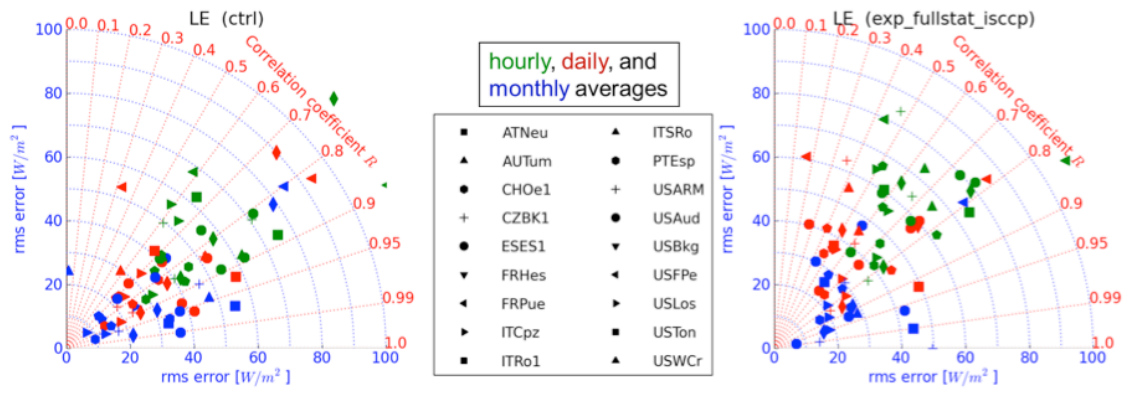


Figure 4: Multiannual RMSE difference and correlation of latent heat flux obtained from station forcing (left) and satellite forcing (right) using different FluxNet stations as a reference. Different colors correspond to different temporal aggregation (Borsche and Loew 2012).

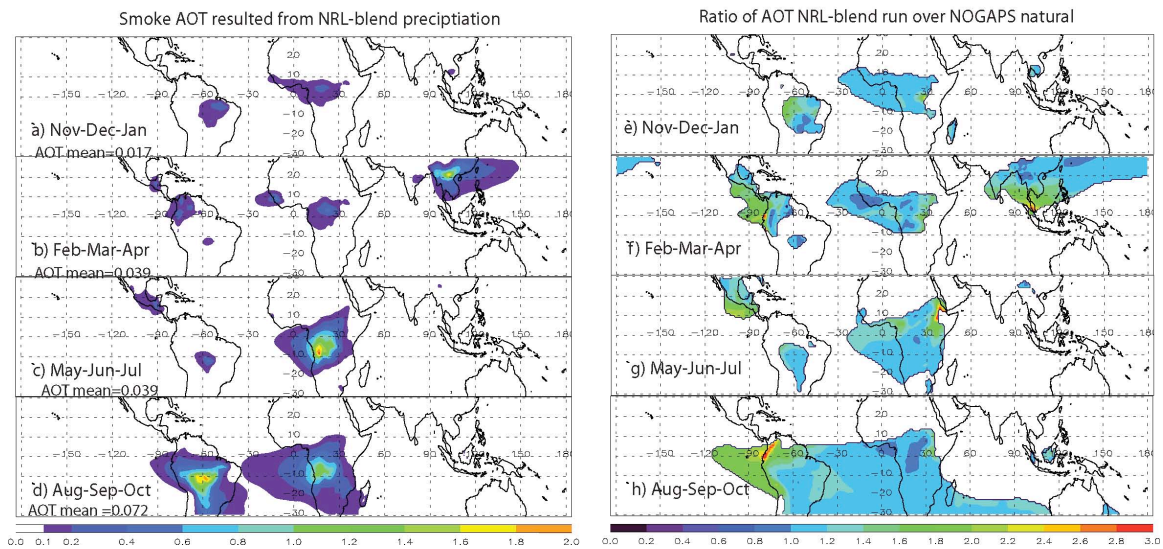


Figure 5: (Left) Smoke AOT resulted from NRL-blend precipitation for four biomass burning periods in 2007. (Right) Ratio of smoke AOT resulted from NRL-blend precipitation over smoke AOT resulted from NOGAPS precipitation for four biomass burning periods in 2007 (colored for regions with AOT > 0.05 in NRL-blend run) (Peng et al. 2009).

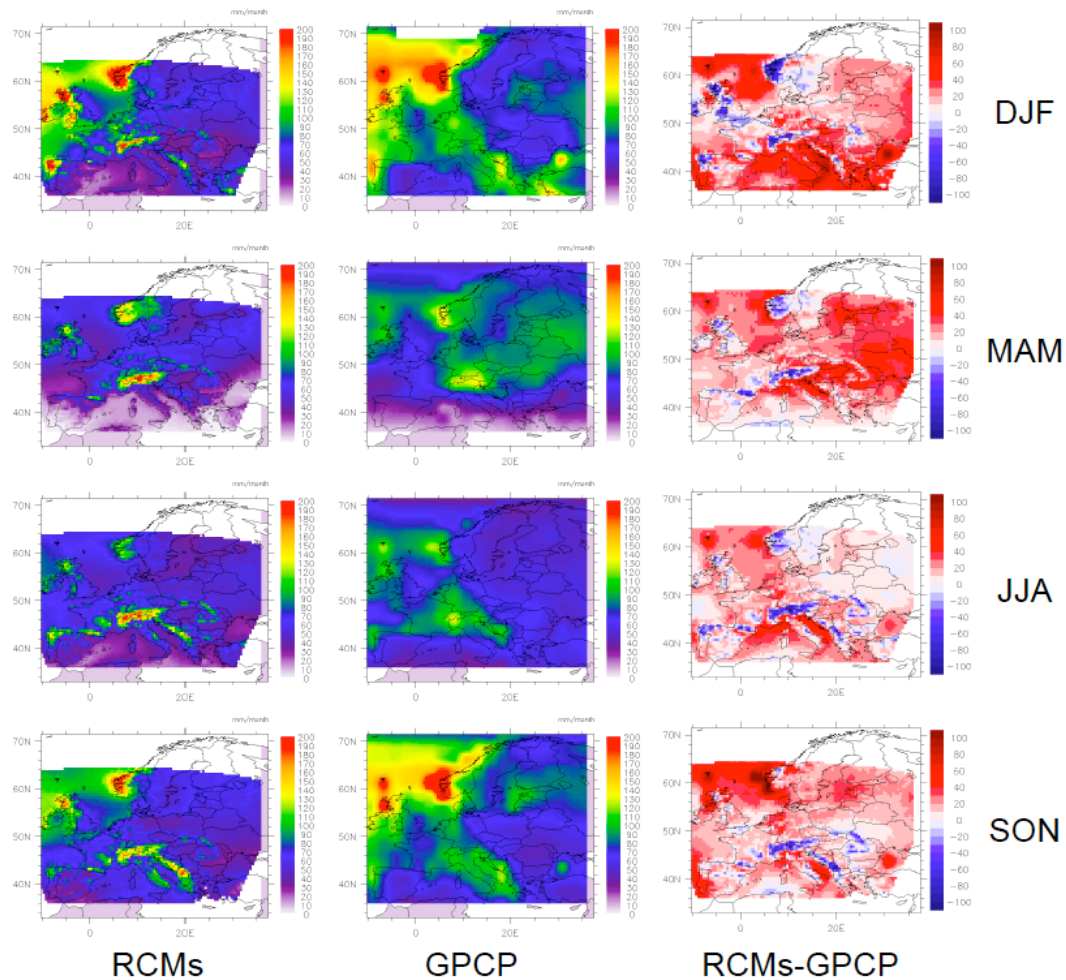


Figure 6: Comparison of the ensemble average of eight Regional Climate Models (RCMs, 0.5° resolution) with a satellite-based observational database (GPCP, 2.5° resolution) over Europe, for present-day climatologies. The difference plots (third column) illustrate the contrasting performances of the RCMs depending on season and on location. Note the different spatial resolution of the data, which affects maxima and minima.

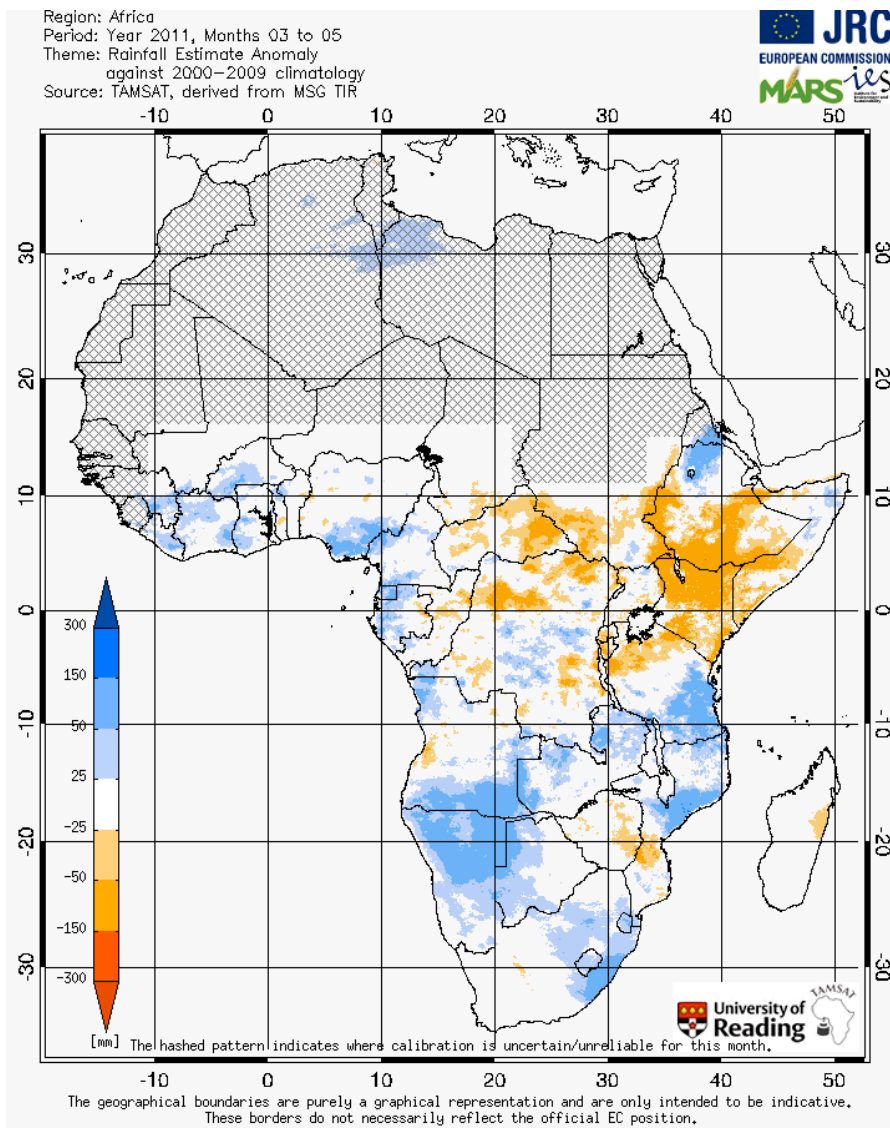


Figure 7: African 2011 MAM rainfall anomaly relative to 2000-2009 climatology.